Residual energy in optical-field-ionized plasmas with the longitudinal motion of electrons included

Bin He and Tie-qiang Chang
Institute of Applied Physics and Computational Mathematics P.O. Box 8009-57, Beijing 100088, People's Republic of China
(Received 26 January 2005; published 30 June 2005)

The space-charge effect on the residual energy of electrons in optical-field-ionized plasmas is studied in detail by an extended simplified model and the cloud-in-cell simulation, with the longitudinal motion of electrons included. It is found that in moderate conditions the space-charge field can influence the residual energy of electrons effectively by matching the space-charge field with laser pulse. The effect of stimulated Raman scattering on electron temperature is also investigated in detail. Finally, a comparison is made between the results and experimental data.

DOI: 10.1103/PhysRevE.71.066411 PACS number(s): 52.50.Jm, 52.38.Dx, 52.65.Rr

I. INTRODUCTION

A cold and dense plasma has a potential for generating soft-x-ray laser [1]. When a beam of intense laser passes through gas, the gas will be ionized and plasma is formed. The electrons in the plasma will move in the pump laser field and the space-charge field induced by the electron motion. After the applied laser pulse vanishes, the electrons would still preserve a part of kinetic energy which is called residual energy. However, for generating the x-ray laser the residual energy must be much lower than the ionization potential, so that the three-body recombination could take place efficiently. The requirements for the conditions of pump laser as well as the laser medium have been investigated theoretically [1–7]. The above-threshold ionization (ATI) induced heating can be decreased by using a short-wavelength pump laser because it is proportional to the square of pump laser wavelength [3], and the temperature of the electrons produced by optical-field-induced ionization (OFI) is lower for linearly polarized laser pulse than for a circularly polarized one [2–5]. In addition, a long pulse laser is preferable to OFI because of being able to decrease the ATI heating [3]. Now the intense lasers for producing the high ionization states are achievable and some experiments have been done to measure the so produced plasma temperature [8–12].

Some authors [3,10] have realized that the residual energy can be reduced by space-charge effect and the harmonic oscillator model has been proposed to describe the electron motion in laser electric field and electrostatic field, in which the space-charge field is taken as a restoring force [3,6],

$$\ddot{y} + \omega_p^2 y = -\frac{e}{m} E_y(y,t). \tag{1}$$

Here $E_y(y,t)$ represents the electric field of the applied laser beam and ω_p is the plasma frequency. Based on this model, Penetrante and Bardsley thought that the presence of space-charge field could significantly lower the residual electron energy by matching plasma frequency ω_p with the pulse width τ_p. Pulsifer *et al.* [6] pointed out that the residual energy of one electron could be reduced to half if the space-charge effect was considered, while the other part would be transferred into the potential energy of the electron. They also pointed out that there would be no significant change of the residual energy with τ_p.

In the investigation of residual energy it was also found that the inverse bremsstrahlung heating [3,6] and stimulated Raman scattering (SRS) [5] were important mechanisms for increasing the plasma temperature. The influence of SRS on the residual energy was estimated in our previous paper [13].

As far as we know, in the discussion of the residual energy the longitudinal motion of electrons (in the direction of the propagation of laser pulse) and the longitudinal electrostatic field are usually neglected. In fact it is not clear whether the longitudinal motion of electrons affects the residual energy. In addition, althrough the influence of SRS on residual energy has been proved negligible in the very low density case, it would become important with the increasing of the electron density n_e. In Sec. II of this paper an extended harmonic oscillator model is proposed to investigate the influence of the longitudinal motion and space-charge field on the residual energy. In Sec. III, a particle simulation code, which has been modified to include the ionization process, is used to simulate the influences of SRS and space charge field on the residual energy in detail. We find out that, in moderate conditions, the residual energy of electrons will be increased effectively if the frequencies of the space-charge field and the laser field are properly matched. Finally, the comparison between the theoretical results and experimental data [9,11] is made in Sec. IV.

II. EXTENDED HARMONIC OSCILLATOR MODEL

As is well known, in the nonrelativistic limit the transverse velocity of the electrons in a laser field is much larger than the longitudinal one. However, with the laser intensity and plasma density increased, the influence of the longitudinal motion would no longer be ignored. In order to clarify this problem we extend the harmonic oscillator model [3,6] by including the longitudinal motion of electrons and longitudinal electrostatic field. Still describing the longitudinal electric field as a harmonic restoring force, Eq. (1) is revised as

$$m\frac{d}{dt}V_y = -eE_y + \frac{e}{c}V_x B_z - m\omega_p^2 y, \tag{2}$$

 ©2005 The American Physical Society

$$m\frac{d}{dt}V_x = -\frac{e}{c}V_y B_z - m\omega_p^2 x, \tag{3}$$

where x and y represent the longitudinal coordinate and the transverse one respectively, V_x and V_y are the corresponding velocities, E_y and B_z denote the electric and magnetic fields of the applied linearly polarized laser. The laser pulse propagates along the x direction. The classical motion equation is still considered since here the movement is only weakly relativistic. The ions are assumed immobile. Obviously, here the effect of SRS is not included.

Above equations cannot be solved analytically and in the following we look for their numerical solution. To calculate the residual energy the ionization must be included and the tunneling ionization model [14] is taken to describe the laser-atom interaction in the strong field [3]. Let $n_j(t)$ be the number density of charge state j at time t, the evolution of $n_j(t)$ is given by the following coupled equations:

$$\dot{n}_0(t) = -W_1(t)n_0(t),$$

$$\dot{n}_j(t) = W_j(t)n_{j-1}(t) - W_{j+1}n_j(t),$$

$$\dot{n}_{zmax}(t) = W_{zmax}(t)n_{zmax-1}(t),$$

where $W_j(t)$ is the ionization rates for the production of charge state j from $j-1$, and

$$W_j(t) = 1.61\omega_{a.u.}\frac{Z^2}{n_{eff}^{4.5}}\left(10.87\frac{Z^3}{n_{eff}^4}\frac{E_{a.u.}}{|E_t|}\right)^{2n_{eff}-1.5} \times e^{-(2/3)(Z^3/n_{eff}^3)(E_{a.u.}/|E_t|)}$$

with

$$n_{eff} = \frac{Z}{(U_j/U_H)^{1/2}}, \quad U_H = 13.6 \text{ eV},$$

$$\omega_{a.u.} = 4.1 \times 10^{16}/\text{s}, \quad E_{a.u.} = 5.1 \times 10^9 \text{ V/cm},$$

where Z is the core charge, U_j is the ionization potential, and E_t the total electric field. In the above equations the recombination process is ignored because the applied intense laser pulse is ultrashort ($\tau_p \ll 1$ ps), whereas the recombination occurs at least after several pulse lengths.

In the calculation residual energy is defined as the final kinetic energy of the electrons after the laser pulse disappears and the electrons are assumed to be born with zero velocity. In our calculations $t=5\tau_p$ is chosen as the time for the pulse to stop. In order to compare the calculated results with experimental data, the residual energy is taken as the average one of all the ionized electrons, and the influence of the space-charge field on the ionization rate is neglected in calculation, as usual. Also, the electromagnetic fields E_y and B_z are chosen to be their vacuum values since the electron density n_e is usually much smaller than the critical one, n_c. We consider helium gas. The maximum intensity and the wavelength of the laser pulse are chosen as $I=10^{18}$ W/cm^2 and $\lambda=248$ nm. The laser pulse is given by

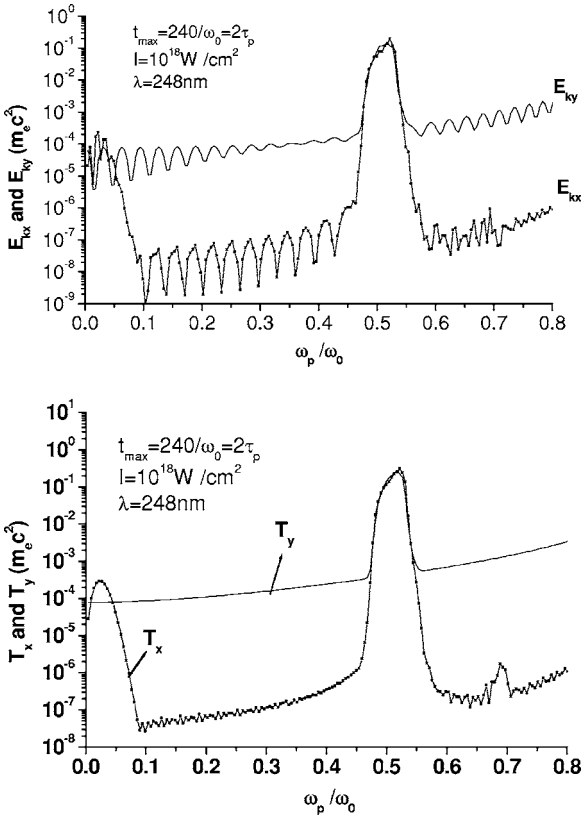

FIG. 1. (a) The dependence of the final kinetic energy $E_{\rm kx}$ and $E_{\rm ky}$ on $\omega_{\rm p}$ from the simple model. (b) The dependence of the final total energy $T_{\rm x}$ and $T_{\rm y}$ on $\omega_{\rm p}$ from the simple model.

$$E_y(t) = E_0 \exp\left[-2\left(\frac{t-t_{max}}{\tau_p}\right)^2\right]\sin\omega_0 t \tag{4}$$

and t_{max} is taken as two times the laser pulse length τ_p. Owing to the similarity of the ionization and motion for all electrons in the laser propagation path (only with a time delay), in the simple model we only consider the motion of the electrons produced at the fixed place where both the initial x and y are equal to zero. The calculation results are shown in Fig. 1, in which both the kinetic energy and total energy of an electron have been divided into two parts corresponding to x and y directions. The average kinetic energy E_k and total energy T are defined as the following:

$$E_{kx} = \frac{1}{N_e}\sum_{i=1}^{N_e}\frac{1}{2}m_e V_{xi}^2, \quad T_x = \frac{1}{N_e}\sum_{i=1}^{N_e}\left(\frac{1}{2}m_e V_{xi}^2 + \frac{1}{2}m_e\omega_p^2 x_i^2\right),$$

$$E_{ky} = \frac{1}{N_e}\sum_{i=1}^{N_e}\frac{1}{2}m_e V_{yi}^2, \quad T_y = \frac{1}{N_e}\sum_{i=1}^{N_e}\left(\frac{1}{2}m_e V_{yi}^2 + \frac{1}{2}m_e\omega_p^2 y_i^2\right).$$

Figures 1(a) and 1(b) show the dependence of the final E_{ky}, E_{kx}, T_y, and T_x on ω_p for $\tau_p=240/\omega_0$. In these figures the kinetic energy is usually one-half of the total energy, which means that the space-charge field can transfer half of the kinetic energy into potential energy on average. Besides, we notice that there are two peaks at $\omega_p \ll \omega_0$ and $\omega_p \sim 0.5\omega_0$. If the peaks are ignored, the residual energy varying with ω_p in

Fig. 1(a) agrees with that described by Eq. (15) in Ref. [6]

$$\epsilon(t_0) \simeq \frac{e^2E^2(t_0)}{4m}\left(\frac{\omega_p^2\sin^2\omega_0 t_0 + \omega_0^2\cos^2\omega_0 t_0}{(\omega_0^2-\omega_p^2)^2}\right).$$

In order to find the location of the first peak of T_x for $\omega_p \ll \omega_0$, many similar calculations have been made for different pulse lengths τ_p. Similar peaks are observed and the location is close to $\omega_p\tau_p \simeq 2.5$. This means that the formation of the peak is closely related to τ_p, in other words, the peak is caused by the resonant match between the pulse profile and the electrostatic field in the x direction. It is natural to think that the peak should have to do with the mechanism of laser wakefield accelerator [15]. As a matter of fact, at the rising stage of the laser pulse the electrons are pushed out of the pulse region by the ponderomotive force, whereas in the descending stage the electrons experience an opposite motion. If the push and pull force on electrons is resonant with Langmuir wave, the Langmuir oscillation will be enhanced. The oscillation will continue even after the pulse disappears and some of its energy will be converted into the longitudinal part of the kinetic energy E_{kx}. Meanwhile, since the oscillation velocity is not very high for nonrelativistic laser intensity and the laser pulse is not very narrow compared to its oscillation period, only a little part of the energy can be transferred into the transverse kinetic energy by Lorentz force. This results in no corresponding peak appearing in T_y in Fig. 1. Another peak is at $\omega_p \simeq 0.5\omega_0$ and it should be the resonant coupling between the two-directed restoring oscillations through Lorentz force. Since the restoring velocity in the y direction has the frequency of $0.5\omega_0$, it induces a frequency component of $0.5\omega_0$ in the longitudinal motion by Lorentz force. This is just the same as the restoring force frequency in the x direction and leads to the resonance exciting very strong oscillation in the direction. For the same reason there exists strong oscillation in the y direction. Consequently, these resonances result in very high residual energy. We have also made some similar calculations without considering the transverse electrostatic field. This time no such peaks are observed, while the peak for $\omega_p\tau_p \simeq 2.5$ still exists. Maybe this can be used as a different mechanism of accelerating electrons, worthy of further investigations.

We also have made a lot of similar computations for different τ_p and obtained similar results. The residual energies corresponding to the two peaks with $\omega_p\tau_p = 2.5$ and $\omega_p = 0.5\omega_0$ are also collected in Figs. 2(a) and 2(b). Figure 2(a) shows the residual energy decreasing with increasing τ_p. The reason is that the shorter the pulse, the more electrons are produced at the time close to the maximum of the pulse intensity, and the stronger the wakefieldlike effect is, consequently, the higher the residual energy becomes. However, the behavior becomes quite different for the $\omega_p \simeq 0.5\omega_0$ peak as shown in Fig. 2(b). In this case the longer the pulse, the longer the time for accelerating the electrons resulting in higher residual energy. Calculations are also made for nonplane electromagnetic wave such as the Gaussian transverse profile of the pulse with different τ_p and the similar behavior is obtained.

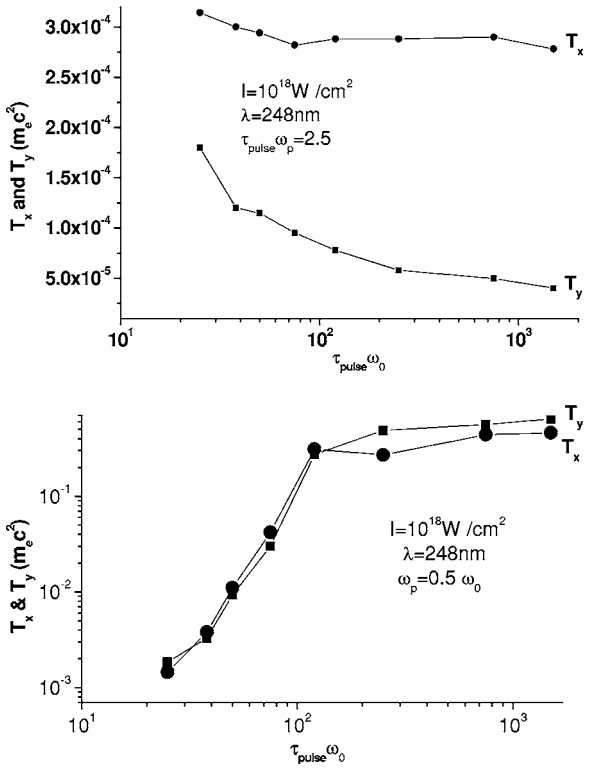

FIG. 2. (a) The dependence of the final total energy T_x and T_y upon τ_{pulse} at $\tau_{\text{pulse}}\omega_p = 2.5$ from the simple model. (b) The dependence of the final total energy T_x and T_y upon τ_{pulse} at $\omega_p = 0.5\omega_0$ from the simple model.

The results lead to the conclusion that the residual energy could be neither reduced significantly by the match between ω_p and τ_p as expected by Penetrante and Bardsley [3], nor little changed with the pulse width as expected by Pulsifer *et al.* [6]. The better view should be that in some special cases the pulse width has effective influence upon the residual energy. However, the results are based on the simple model, in which the influence of SRS is not included, and the results should also be checked by particle simulation, which will be discussed in the next section.

III. PARTICLE SIMULATION OF RESIDUAL ENERGY

Because the ionization occurs at different locations and different times, the laser-ionized electrons are subjected to different forces from the laser pulse and the interactions among them are complicated. So the problem should be studied by computer simulation with a cloud-in-cell (CIC) code. In the method the real particles are replaced by some clouds, their motions are governed by the Lorentz equation, and the Maxwellian equations for electric and magnetic fields are simultaneously solved. There are some good introductions to the CIC or the PIC (particle-in-cell) methods [16]. For present purposes our one-dimensional (1D) relativistic CIC code [17] with nonperiodic boundary condition is revised to include the ionization process according to the previous scheme [14]. However, this kind of code could not describe the residual energy related to the transverse electrostatic

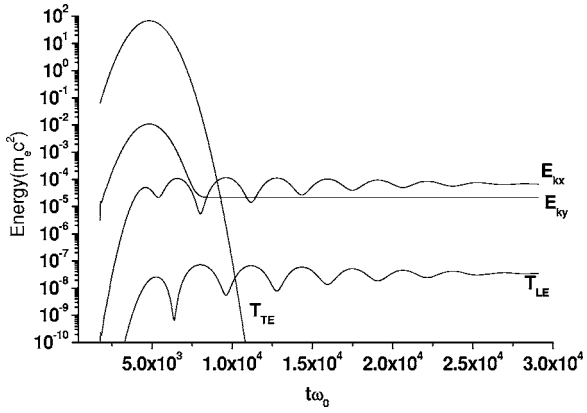

FIG. 3. The evolution of the various energy when $n_{\mathrm{He}}=0.9\times10^{16}$ cm^3 from PIC. Here $I=10^{18}$ W/cm^2, $\lambda=248$ nm, and $t_{\max}=2\tau_{\mathrm{pulse}}=4500/\omega_0$.

field. So the results obtained by the simple model and 1D CIC code should be combined to get a more complete understanding.

The following two points about the simulation should be declared:

(i) The linearly polarized electromagnetic wave propagates in the x direction with wavelength 248 nm and maximum intensity 10^{18} W/cm^2. The electric field of the incident pulse is described by Eq. (4). The simulation system is 100λ long with helium gas situated in the middle, which is 20λ long. The rest of the system at the initial time is vacuum so as to make the electrons arriving at the system boundaries as few as possible and the results more accurate.

(ii) The time step δt and spatial step δx is related by $\delta x=c\delta t$ and δt is less than $0.1/\omega_0$. All the electrons are born with zero velocity. The ions are immobile. Specular reflection is chosen for the particles hitting the boundary. A total of about several 10^5 particles are produced and simulated in each run.

Figure 3 shows the time evolution of the transverse part of the field energy T_{TE}, the longitudinal part T_{LE}, the average transverse kinetic energy E_{ky}, the average longitudinal one E_{kx}, and the total energy T_E of the system. Here the following definitions are given:

$$T_{TE}=\sum_{j=1}^{NX}[E_y^2(j)+B_z^2(j)],\quad T_{LE}=\sum_{j=1}^{NX}E_x^2(j),$$

$$E_{ky}=\frac{1}{2N_e}\sum_{i=1}^{N_e}m_eV_{yi}^2,\quad E_{kx}=\frac{1}{2N_e}\sum_{i=1}^{N_e}m_eV_{xi}^2,$$

where NX is the total number of spatial grids, N_e the total number of the ionized electrons, and E_x is the longitudinal electrostatic field. In the figure τ_p is fixed at 300 fs and the helium gas density n_{He} is 0.9×10^{16}/cm^3. From Fig. 3 it can be found that the evolution of E_{ky} and T_{TE} agree with that of the laser pulse, as they should be. The final E_{ky} is very close to that obtained by the harmonic oscillator model without electrostatic field, which indicates that our results of simulation are reasonable. The final E_{kx} is about three times E_{ky}.

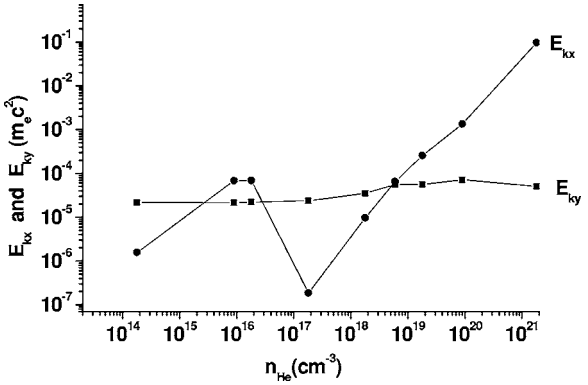

FIG. 4. The dependence of the kinetic energy E_{kx} and E_{ky} upon the density of helium gas n_{He} from PIC. Here $I=10^{18}$ W/cm^2, $t_{\max}=2\tau_{\mathrm{pulse}}=4500/\omega_0$, and $\lambda=248$ nm.

This is because of the resonant condition $\omega_p\tau_p=2.5$ which is satisfied since helium gas is double ionized. This resonance agrees well with the results obtained by the previous simple model. In addition, no signal of SRS is observed because of too low electron energy of $2\times10^{-6}n_c$. We also carried out some other simulations with different n_e in similar conditions and the results are collected in Fig. 4. The figure shows that E_{ky} gradually increases with n_{He} because SRS gradually becomes strong. For n_e of the order of 10^{14}/cm^3 E_{kx} is very small since there is neither SRS nor the match between τ_p and ω_p. However, in the vicinity of 10^{16}/cm^3 of n_{He}, E_{kx} becomes high, that should be induced by the mentioned match. Then, E_{kx} becomes small again until n_{He} reaches about 10^{18}/cm^3 above which SRS starts to play a more and more important role, hence higher and higher E_{kx}. For $n_e=0.9\times10^{20}$/cm^3 the anti-Stokes wave induced by SRS with frequency of $\omega_0-\omega_p$ is clearly observed (not shown here). No further simulation is performed with n_e exceeding $0.25n_c$ where no SRS occurs.

Some simulations for other τ_p are also performed and similar behaviors to those in Figs. 3 and 4 are obtained. Figures 5 and 6 show similar results for τ_p equal to 100 and 3.5 fs, respectively. The comparison among these figures suggests that E_{ky} becomes higher with shorter pulse, which

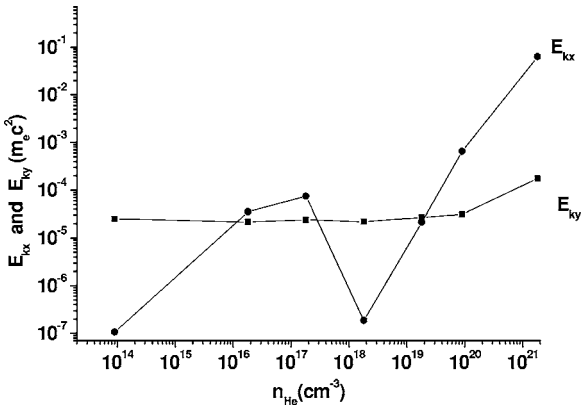

FIG. 5. The dependence of the kinetic energy E_{kx} and E_{ky} upon the density of helium gas n_{He} from PIC. Here $I=10^{18}$ W/cm^2, $t_{\max}=2\tau_{\mathrm{pulse}}=1500/\omega_0$, and $\lambda=248$ nm.

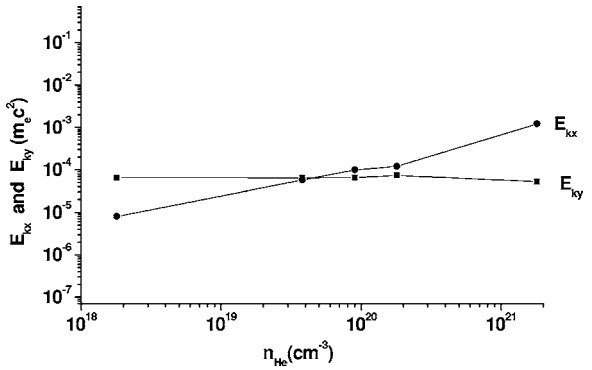

FIG. 6. The dependence of the kinetic energy E_{kx} and E_{ky} upon the density of helium gas n_{He} from PIC. Here $I=10^{18}$ W/cm^2, $t_{max}=2\tau_{pulse}=50/\omega_0$, and $\lambda=248$ nm.

agrees with the results in the last section. It also indicates that the longer the laser pulse is, the more intense SRS becomes, hence the higher residual E_{kx}.

IV. COMPARISON WITH EXPERIMENTAL DATA

In this section some comparisons are made between experimental data and our results. Several years ago Glover *et al.* [9] measured the temperature of electrons in plasmas formed by intense laser incident upon helium gas with density no less than 10^{18}/cm^3. Table I shows the experimental data and our simulation results. In the following the electron temperature is defined as $\varepsilon_e=\frac{2}{3}(E_{kx}+E_{ky})$. It should be noticed that our simulation results for E_{ky} have been divided by 2 for considering the effect of the transverse electrostatic field.

In Table I T_e represents the measured electron temperature. It is seen that our results are consistent with the experimental data and SRS plays an important role.

TABLE I. Glover *et al.* experimental data and simulation results.

I (W/cm^2)	2×10^{16}	2×10^{17}
τ_p (fs)	160	125
λ (nm)	616	800
T_e (eV)	22±4	40–50
ε_e (eV)	23	38
$\frac{2}{3}E_{ky}$ (eV)	17	28
$\frac{2}{3}E_{kx}$ (eV)	6	10

TABLE II. Blyth *et al.* experimental data and our results.

n_e (cm^3)	3×10^{17}	3×10^{18}	1.2×10^{19}
T_e (eV)	6.0±3.0	10.0±6.0	30.0±15.0
ε_e (eV)	4.4	5.0	50
$\frac{2}{3}E_{ky}$ (eV)	4.0	4.5	16
$\frac{2}{3}E_{kx}$ (eV)	<0.4	<0.5	34

Similarly Blyth *et al.* [11] measured the electron temperature with helium gas. The following is the experimental condition:

$$I=10^{18}\ \text{W/cm}^2,\quad \lambda=248\ \text{nm},\quad \tau_p=350\ \text{fs}.$$

We also made the corresponding simulations and the comparison displayed in Table II.

Table II shows that the comparison is satisfactory. With n_e increasing, the residual energy becomes much higher and SRS becomes very important.

In conclusion, we have proposed an extended harmonic oscillator model to investigate the influence of the electrostatic field and the longitudinal motion of electrons on residual energy. In order to clarify the influence of SRS and longitudinal electrostatic field, we have also performed some particle simulation and made comparisons with the experimental data. Finally the following conclusions can be drawn:

(i) Under moderate matching condition, we mean $\tau_p\omega_p\simeq2.5$, a kind of resonance related to the laser wakefield occurs even for very low n_e, which results in the effective increasing of longitudinal part of residual energy.

(ii) When $\omega_p\simeq0.5\omega_0$ another kind of resonance takes place in both the transverse and longitudinal direction, which gives rise to very high residual energy.

(iii) In the case of n_e much lower than n_c, the longitudinal motion of electrons has little influence on residual energy if no matching condition mentioned above is satisfied.

(iv) With n_e increasing SRS becomes strong and has strong influence upon residual energy.

(v) The transverse part of residual energy becomes higher with shortening laser pulse, whereas the longitudinal one becomes higher with lengthening laser pulse.

ACKNOWLEDGMENTS

This work was supported by Science and Technology Funds of China Academy of Engineering Physics by Grant No. 980226, the National Natural Science Foundation of China under Grant No. 19735002, and National High-Tech. ICF Committee in China.

[1] J. Peyroud and N. Peyroud, J. Appl. Phys. **43**, 2993 (1972); W. W. Jones and A. W. Ali, Appl. Phys. Lett. **26**, 450 (1975).

[2] N. H. Burnett and P. B. Corkum, J. Opt. Soc. Am. B **6**, 1195 (1989); N. H. Burnett and G. D. Enright, IEEE J. Quantum Electron. **QE-26**, 1797 (1990).

[3] B. M. Penetrante and J. N. Bardsley, Phys. Rev. A **43**, 3100 (1991).

[4] P. Agostini, F. Fabre, G. Mainfray, G. Petite, and N. K. Rahman, Phys. Rev. Lett. **42**, 1127 (1979); R. R. Freeman, P. H. Bucksbaum, H. Milchberg, S. Darack, D. Schumacher, and M. E. Geusic, *ibid.* **59**, 1092 (1987); T. F. Gallagher, *ibid.* **61**, 2304 (1988); P. B. Corkum, N. H Burnett, and F. Brunel, *ibid.*

62, 1259 (1989).
[5] D. C. Eder, P. Amendt, and S. C. Wilks, Phys. Rev. A **45**, 6761 (1992); S. C. Wilks, W. L. Kruer, E. A. Williams, P. Amendt, and D. C. Eder, Phys. Plasmas **2**, 274 (1995).
[6] P. Pulsifer *et al.*, Phys. Rev. A **49**, 3958 (1994).
[7] T. J. McIlrath, P. H. Bucksbaum, R. R. Freeman, and M. Bashkansky, Phys. Rev. A **35**, 4611 (1987); W. P. Leemans, C. E. Clayton, W. B. Mori, K. A. Marsh, P. K. Kaw, A. Dyson, C. Joshi, and J. M. Wallace, *ibid.* **46**, 1091 (1992).
[8] U. Mohideen, M. H. Sher, H. W. K. Tom, G. D. Aumiller, O. R. Wood II, R. R. Freeman, J. Boker, and P. H. Bucksbaum, Phys. Rev. Lett. **71**, 509 (1993).
[9] T. E. Glover, T. D. Donnelly, E. A. Lipman, A. Sullivan, and R. W. Falcone, Phys. Rev. Lett. **73**, 78 (1994).
[10] Yutaka Nagata, Katsumi Midorikawa, Shoich Kubodera, Minoru Obara, Hideo Tashiro, Koichi Toyoda, and Y. Kato, Phys. Rev. A **51**, 1415 (1995).
[11] W. J. Blyth, S. G. Preston, A. A. Offenberger, M. H. Key, J. S. Wark, Z. Najmudin, A. Modena, A. Djaoui, and A. E. Dangor, Phys. Rev. Lett. **74**, 554 (1995).
[12] Yutaka Nagata, Katsumi Midorikawa, Shoich Kubodera, Minoru Obara, Hideo Tashiro, and Koichi Toyoda, Phys. Rev. Lett. **71**, 3774 (1993).
[13] Bin He, Tie-qiang Chang, Shi-gang Chen, Xiao-bo Nie, Jia-tai Zhang, and Lin-bao Xu, J. Phys. D **30**, 400 (1997).
[14] M. V. Ammosov, N. B. Delone, and V. P. Krainov, Zh. Eksp. Teor. Fiz. **91**, 2008 (1986) [Sov. Phys. JETP **64**, 1191 (1986)].
[15] P. Chen, J. M. Dawson, R. W. Huff, and T. Katsouleas, Phys. Rev. Lett. **54**, 693 (1985).; E. Esarey, A. Ting, P. Sprangle, and G. Joyce, Comments Plasma Phys. Controlled Fusion **12**, 191 (1990).
[16] W. L. Kruer, *The Physics of Laser Plasma Interactions* (McGraw-Hill, New York, 1981); C. K. Birdsall and A. B. Longdon, *Plasma Physics via Computer Simulation* (McGraw-Hill, New York, 1985).
[17] L. B. Xu, Fusion and Plasma Physics (in Chinese) **V2**, 92 (1982); J. T. Zhang, Commun. Theor. Phys. **3**, 243 (1986); **4**, 543 (1990).